Surface Structure and Temperature Dependence of Light-Alkane Skeletal Rearrangement Reactions Catalyzed over Platinum Single-Crystal Surfaces

S. Mark Davis,† Francisco Zaera, and Gabor A. Somorjai*

Contribution from the Department of Chemistry, University of California, Berkeley, and Materials and Molecular Research Division, Lawrence Berkeley Laboratory, Berkeley, California 94720. *Received March 11, 1982*

Abstract: The structure sensitivity of isobutane, *n*-butane, and neopentane hydrogenolysis and isomerization catalyzed over a series of flat, stepped, and kinked platinum single-crystal surfaces was investigated near atmospheric pressure and at 540–640 K. The atomic structure and surface composition of the active catalyst were determined before and after reaction studies by using low-energy electron diffraction and Auger electron spectroscopy. Catalytic activities for butane isomerization and consecutive rearrangement reactions were maximized on platinum surfaces with high concentrations of (100) microfacets. Maximum rates for the competing hydrogenolysis reactions were obtained on platinum surfaces that contain high concentrations of steps and kinks. Hydrogenolysis product distributions varied markedly with terrace structure. The symmetries of d orbitals that emerge from the surfaces with different atomic structure have been used to rationalize the structure sensitivity of light-alkane isomerization.

Skeletal isomerization of C_4 alkanes is perhaps the simplest class of metal-catalyzed hydrocarbon rearrangement reactions. Among all group 8 metals, platinum is a uniquely selective catalyst for these intriguing, intramolecular rearrangements.[1,2] The extraordinary catalytic behavior of platinum has been attributed to several factors including the d spacing of the metal[3] and the positions and occupancies of the almost-filled platinum d bands, which allows for easy electron promotion to form higher energy electronic states.[4,5] A more complete understanding of this reaction chemistry at a predictive level will require detailed information about the structure sensitivity of the reaction pathway on an atomic scale that may serve as a basis for further theoretical analysis. Unfortunately, all previous investigations of metal-catalyzed isomerization reactions have been carried out with practical catalysts (i.e., films, powders, and supported catalysts) where the surface structure was heterogeneous or the surface composition was not known. To circumvent these difficulties, we developed experimental techniques in this laboratory[6] that permit the kinetics of catalyzed reactions to be investigated on small-area metal single-crystal surfaces that possess well-defined atomic structure and surface composition. This report describes studies of *n*-butane, isobutane, and neopentane skeletal rearrangement reactions catalyzed on a series of six platinum single-crystal surfaces with variable terrace, step, and kink structures. The studies were carried out near atmospheric pressure at temperatures between 540 and 640 K. The structure and composition of the active catalyst surface was determined before and after reaction studies using low-energy electron diffraction (LEED) and Auger electron spectroscopy (AES).

We have discovered that the flat (100) and stepped (13,1,1) platinum surfaces that contain high concentrations of square (100) microfacets display an exceptional ability to catalyze bond-shift rearrangement in simple alkanes. Maximum rates for the competing hydrogenolysis reactions that require C–C bond rupture were obtained on stepped and kinked platinum surfaces with terraces of (111) orientation. Hydrogenolysis product distributions varied markedly with terrace structure. A simple geometrical model, based on the symmetries of surface d orbitals, is proposed to interpret the structure sensitivity of light-alkane skeletal rearrangement.

Experimental Section

All of the experiments were carried out in an ultrahigh-vacuum high-pressure apparatus described previously[6] that is designed for combined surface analysis and catalysis studies using small-area catalyst samples. This system was equipped with four-grid electron optics for low-energy electron diffraction (LEED) and Auger electron spectroscopy (AES), an argon ion gun for crystal cleaning, a quadrupole mass spectrometer, and a retractable internal isolation cell, which operates as a well-mixed microbatch reactor in the 10^{-2}–10-atm pressure range. The reaction cell and external recirculation loop were connected to an isolable Wallace & Tiernan guage, a bellows pump for gas circulation, and a gas chromatograph sampling valve. Hydrocarbon conversion was monitored with an HP3880 gas chromatograph calibrated with CH_4/N_2 mixtures.

Idealized atomic surface structures for the six single-crystal samples used in this research are shown in Figure 1. Miller indices, average terrace widths, kink concentrations, and microfacet indices for the various samples are summarized in Table I. In the microfacet notation,[7] the terms $a_b(hkl)$ describe the number b and type (hkl) of terrace, step, and kink microfacets contained in the unit cell of the surface. Flat, stepped, or kinked surfaces are conveniently represented by one, two, or three terms, respectively.[2,7] All the single-crystal samples were prepared[8] as thin (≤0.5 mm) disks so that the polycrystalline edges would contribute no more than 10–16% of the total platinum surface area (≈1 cm²). The total area was used in the calculation of all reaction rates. Research

Table I. Miller Indices, Average Terrace Widths, and Microfacet Indices for Platinum Single-Crystal Surfaces

Miller index	terrace width, Å	microfacet index[a]
Pt(100)		Pt(100)
Pt(111)		Pt(111)
Pt(332)	14.0	Pt(S) – $[(5/2)_5(111) + 1_1(11\bar{1})]$
Pt(557)	13.2	Pt(S) – $[5_5(111) + 2_1(100)]$
Pt(13,1,1)	18.0	Pt(S) – $[12_6(100) + 1_1(111)]$
Pt(10,8,7)[b]	15.1	Pt(S) – $[(15/2)_{15}(111) + 2_2(100) + 1_1(11\bar{1})]$

[a] For a detailed explanation see ref 7. [b] Kink concentration = 1×10^{14} atom cm^{-2} (i.e., ~6% kinks).

† Permanent address: Exxon Research and Development Laboratory, Baton Rouge, LA 70821.

(1) J. R. Anderson and N. R. Avery, *J. Catal.*, **5**, 446 (1966).
(2) S. M. Davis and G. A. Somorjai in "The Chemical Physics of Solid Surfaces and Heterogeneous Catalysis", Elsevier, Amsterdam, 1981, Vol. 4.
(3) Z. Paal and P. Tetenyi, *Nature (London)*, **267**, 234 (1977).
(4) M. Boudart and L. D. Ptak, *J. Catal.*, **16**, 90 (1970).
(5) D. K. Anderson, *Phys. Rev. B: Solid State*, **2**, 883 (1970); K. A. Mills, R. F. Davis, S. D. Kevan, G. Thornton, and D. A. Shirley, *Phys. Rev. B: Condensed Matter*, **22**, 581 (1980); M. M. Traum and N. V. Smith, *Phys. Rev. B: Solid State*, **9**, 1350 (1974); N. V. Smith, *ibid.*, **9**, 1365 (1974); N. V. Smith, G. K. Wertheim, S. Hufner, and M. M. Traum, *ibid.*, **10**, 3197 (1974).
(6) D. W. Blakely, E. Kozak, B. A. Sexton, and G. A. Somorjai, *J. Vac. Sci. Technol.*, **13**, 1901 (1976).
(7) M. A. Van Hove and G. A. Somorjai, *Surf. Sci.*, **92**, 489 (1980).
(8) S. M. Davis, Ph.D. Thesis, University of California, Berkeley, 1981.

0002-7863/82/1504-7453$01.25/0

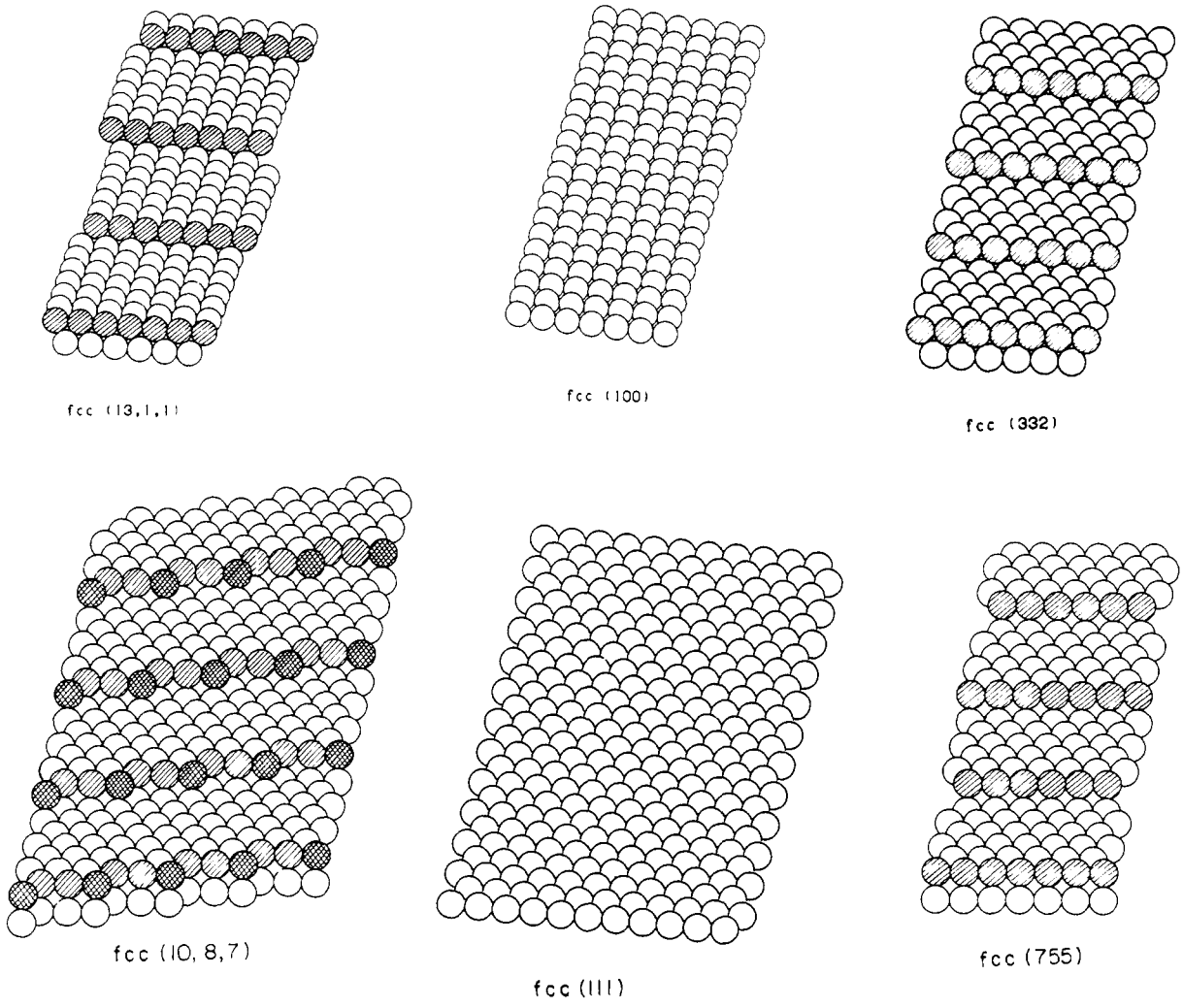

Figure 1. Idealized atomic surface structures for the flat (100) and (111), stepped (332), (557), and (13,1,1), and kinked (10,8,7) platinum single-crystal surfaces.

purity hydrocarbons (Matheson, ≥99.99 mol %) and hydrogen (LBL-Matheson, ≥99.998%) were used as supplied.

The single crystals were spotwelded to a rotatable manipulator by using a series of platinum, gold, and copper supports[9] that enabled the samples to be resistively heated to about 1400 K without significant heating of any other part of the reaction chamber. Both crystal faces were cleaned by using repeated cycles of argon ion sputtering, oxygen pretreatment, and annealing at 1050–1350 K, until the surface structure was well defined by LEED and surface impurities such as Ca, Si, P, S, O, and C were no longer detectable by AES. Subsequently, the reaction cell was closed in seconds and pressurized to about 1 atm with H_2 to cool the sample and supports below 330 K. After about 1 min, the hydrogen was removed, hydrocarbon vapor and hydrogen were reintroduced to desired presssures, circulation was commenced, and the crystal was heated to the reaction temperature over a period of about 1 min. The reaction temperature was continuously regulated to ±2 K with a precision temperature controller referenced to a chromel–alumel thermocouple (tc) spotwelded to an edge or face of the crystal. Since anything but excellent thermal and electrical contact between the tc junction and the crystal would cause the temperature to be underestimated, it was of paramount importance to establish the accuracy of the temperature measurements. The first test used for this purpose was a visual check described by Gillespie.[9] When the thermocouple was properly attached, the threshold temperature for observing visible emission in a dark laboratory was 785 ± 10 K. Studies of isobutane dehydrogenation catalyzed on the single-crystal surfaces provided a second method for establishing the sample temperature under reaction conditions. As discussed below, the dehydrogenation reaction yielded equilibrium concentrations of isobutene under all reaction conditions. In Figure 2 the equilibrium isobutene to

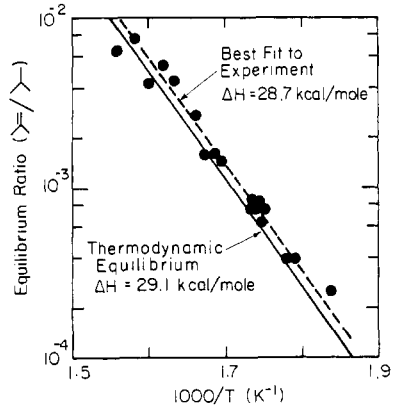

Figure 2. Temperature dependence of the equilibrium ratio of isobutene to isobutane showing the excellent agreement between experimental data and thermodynamic predictions.[10] This comparison provides a simple method to test the absolute sample temperature under reaction conditions (H_2/HC = 10, P_{tot} = 220 torr).

isobutane yields determined in reaction-rate experiments are compared as a function of $1/T$ with the theoretical yields that were calculated from published thermodynamic data (ΔH = 29.1 kcal/mol).[10] The agreement between temperature scales was generally excellent, although near 573 K there was a systematic tendency for the experimental isobutene yields

(9) W. D. Gillespie, R. K. Herz, E. E. Pettersen, and G. A. Somorjai, *J. Catal.* **70**, 147 (1981).

(10) D. R. Stull, E. F. Westrum, and G. C. Sinke, "The Chemical Thermodynamics of Organic Compounds", Wiley, New York, 1969.

Table II. Initial Reaction Rates, Selectivities, and Carbon Coverages Determined for Isobutane Reactions Catalyzed at 573 K over Platinum Single-Crystal Surfaces[a]

catalyst	initial rates at 573 K, molec/Pt·atom·s (±20%)			activation energy, kcal/mol		selectivity of isom,[b] mol %	C/Pt,[c] (±25%)
	hydrog	isom	dehydrog	hydrog	isom		
Pt(100)	0.0047	0.22	≳0.5	35	15	98	1.1
Pt(111)	0.0036	0.032	≳0.4			90	1.5
Pt(13,1,1)	0.0055	0.20	≳0.4			97	1.2
Pt(10,8,7)	0.014	0.060	≳0.9	16	13	81	1.4
Pt(557)	0.014	0.10	≳0.8			88	1.7
Pt(332)	0.0097	0.062	≳0.3			86	1.0

[a] $H_2/HC = 10$, $P_{tot} = 220$ torr. [b] $S_{isom} = R_{isom}/(R_{isom} + R_{hydrog})$. [c] Carbon atoms per surface Pt atom.[8,13]

to exceed the expected yields by 5–18%. This difference corresponds to an error in the temperature measurement of 2–5 K, which might be expected if (1) conductive losses take place at the crystal–thermocouple junction or (2) the temperature of the crystal–support contacts was slightly hotter than that for the sample itself. The samples were repeatedly mounted and remounted until the heating was uniform and the contact points (about 2–3% of the total platinum area) appeared to be no hotter than the sample itself. These methods were essential to insure that the crystal temperature was closely standardize from one sample to the next.

At the end of the reaction-rate studies, the samples were cooled to below 320 K, the reaction mixture was removed, the reaction cell was opened, and Auger spectra were immediately recorded, all within a period of about 5–20 min. Contamination of the surface by impurities such as sulfur and chlorine was not observed following butane and *n*-hexane reaction studies, although *low* levels of sulfur contamination were always detected following neopentane reactions. This sulfur appeared to be deposited rapidly (within minutes) as the reaction commenced. Approximate sulfur coverages expressed as sulfur atoms per surface platinum atom were estimated from AES peak-to-peak heights by using $S/Pt = 0.02\ [S_{152}/Pt_{237}]$.[8]

Initial reaction rates were determined graphically from the slopes of product accumulation curves determined as a function of reaction time. Initial rates and selectivities were reproducible to about ±20% and ±5%, respectively. Blank reaction studies, carried out over surfaces covered with graphitic carbon deposits that formed upon heating in hydrocarbon at 750–800 K, revealed a very low level of background catalytic activity corresponding to 2–4% of the activity measured for initially clean platinum.

It is important to note that the clean (100) and (13,1,1) platinum crystal faces display surface reconstructions that can be approximately represented by (5 × 20) coincidence lattice structures.[11,12] Dynamical LEED intensity calculations[12] for Pt(100) have revealed that the topmost surface layer is hexagonal, buckled, and contracted about 6% with respect to the bulk metal d spacing. Upon exposure to hydrocarbons at high or low pressures, we have always observed (1 × 1) structures indicative of the unreconstructed (100) and (13,1,1) crystal faces. Since hydrocarbon catalysis appears to occur on these unreconstructed surfaces, the (1 × 1) structures are shown in Figure 1 and will be used in all following discussions.

Results

Isobutane Reactions. The isomerization, hydrogenolysis, and dehydrogenation reactions of isobutane were investigated over the six flat, stepped, or kinked platinum surfaces at temperatures between 540 and 640 K. Standard pressures used for these reaction studies were 20 torr of isobutane and 200 torr of hydrogen. Product accumulation curves determined as a function of reaction time for isobutane isomerization and hydrogenolysis catalyzed at 573 K are compared for the six platinum surfaces in Figure 3. Initial reaction rates and fractional isomerization selectivities ($S_{isom} = R_{isom}/(R_{isom} + R_{hydrog})$) calculated from these data are summarized together with carbon coverages determined by AES[8,11] following a 90–150-min reaction time in Table II. Hydrogenolysis and isomerization both displayed significant structure sensitivity. Differences in initial rates between the least- and most-active crystal faces varied from a factor of 4 for hydrogenolysis to over a factor of 6 for isomerization. The order of activities for isomerization followed the sequence Pt(100) ≈ Pt(13,1,1) > Pt(557) > Pt(10,8,7) ≈ Pt(332) > Pt(111), while the hydrogenolysis rates decreased in the order Pt(557) ≈ Pt(10,8,7) ≈ Pt(332) > Pt(13,1,1) ≈ Pt(100) ≈ Pt(111).

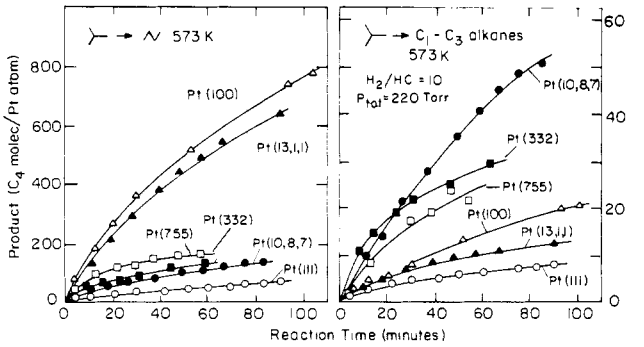

Figure 3. Product accumulation curves determined as a function of reaction time at 573 K for isobutane isomerization (left) and hydrogenolysis (right) catalyzed over platinum single-crystal surfaces.

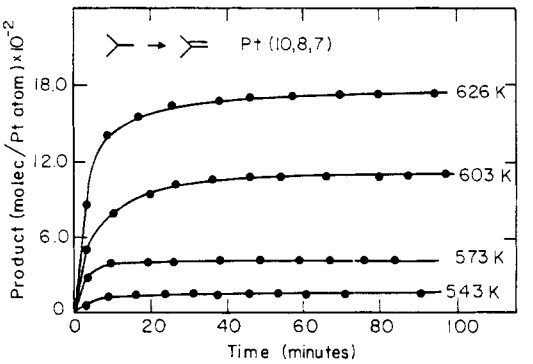

Figure 4. Product accumulation curves determined at several temperatures ($H_2/HC = 10$, $P_{tot} = 220$ torr) for isobutane dehydrogenation catalyzed over the kinked (10,8,7) platinum surface.

Isobutane dehydrogenation produced equilibrium concentrations of isobutene within minutes over all six platinum surfaces under all reaction conditions. Product accumulation curves for the dehydrogenation reaction catalyzed on the (10,8,7) platinum surface are shown at several reaction temperatures in Figure 4. Since the dehydrogenation reaction was already close to equilibrium when the first gas samples were injected into the gas chromatograph, initial dehydrogenation rates could not be determined accurately. As such, the apparent dehydrogenation rates included in Table II represent a lower limit to the actual dehydrogenation rate. Despite these thermodynamic constraints, it is clear from Table II that dehydrogenation was at least 2–6 times faster than isomerization and hydrogenolysis.

Arrhenius plots for isobutane isomerization and hydrogenolysis catalyzed on the (100) and (10,8,7) platinum surfaces are compared in the lower half of Figure 5. Apparent activation energies estimated for reaction temperatures below about 600 K are included in Table II. The temperature dependence of the isom-

(11) D. W. Blakely and G. A. Somorjai, *Surf. Sci.*, **65**, 419 (1977).
(12) M. A. Van Hove, R. J. Koestner, P. C. Stair, J. P. Biberian, L. L. Kesmodel, and G. A. Somorjai, *Surf. Sci.* **103**, (a) 189, (b) 218 (1981).
(13) S. M. Davis, B. E. Gordon, M. Press, and G. A. Somorjai, *J. Vac. Sci. Technol.*, **19**, 231 (1981).

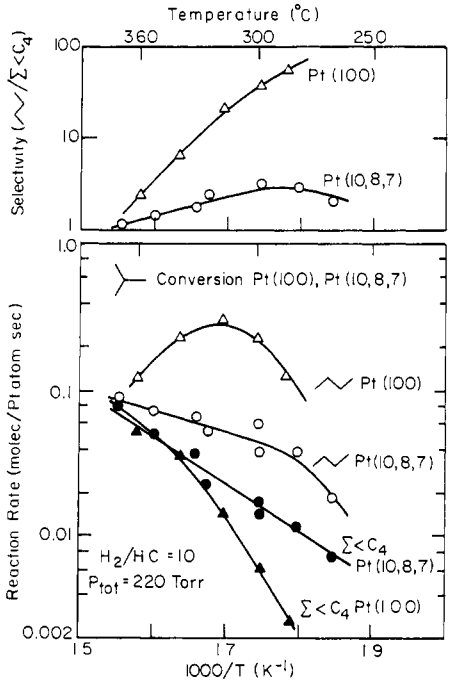

Figure 5. Arrhenius plots (lower) and kinetic selectivities (upper) for isobutane isomerization and hydrogenolysis catalyzed over the flat (100) and kinked (10,8,7) platinum single-crystal surfaces.

Table III. Product Distributions for Isobutane Hydrogenolysis Catalyzed over Platinum Single-Crystal Surfaces[a]

surface	T, K	hydrog dist, mol C_1	C_2	C_3
Pt(100)	561	43	31	6
	573	40	38	22
	590	34	40	26
	611	40	36	24
	633	28	44	28
Pt(13,1,1)	573	30	48	22
Pt(332)	573	70	15	15
Pt(111)	573	55	11	34
Pt(10,8,7)	543	65	6	29
	573	64	10	26
	603	71	7	22
	603	71	10	24
	643	67	10	23
Pt(557)	573	56	5	39

[a] $H_2/HC = 10$, $P_{tot} = 220$ torr.

erization and hydrogenolysis rates was markedly different on the two platinum surfaces. Isomerization activity on Pt(100) displayed a maximum at about 600 K and then decreased with increasing temperature. The activation energy for hydrogenolysis was a substantial 35 ± 5 kcal/mol. The (10,8,7) platinum surface displayed lower activation energies (12–18 kcal/mol) for both reactions, and no rate maxima were detected as a function of temperature.

The kinetic selectivity for isomerization and hydrogenolysis is shown as a function of temperature for the (100) and (10,8,7) platinum surfaces in the upper half of Figure 5. The isomerization selectivity was maximized at low temperatures and decreased drastically with increasing temperatures above about 580 K. Isomerization selectivity on the (100) surface displayed a maximum value of 57 at 560 K that was about 14 times higher than that for Pt(10,8,7). At the highest temperatures studied (≥620 K), the initial rates of isomerization and hydrogenolysis tended to become equal on both surfaces.

Product distributions for isobutane hydrogenolysis catalyzed at 540–640 K over the six platinum surfaces are compared in Table III. Fission parameters[14] calculated from these distributions by

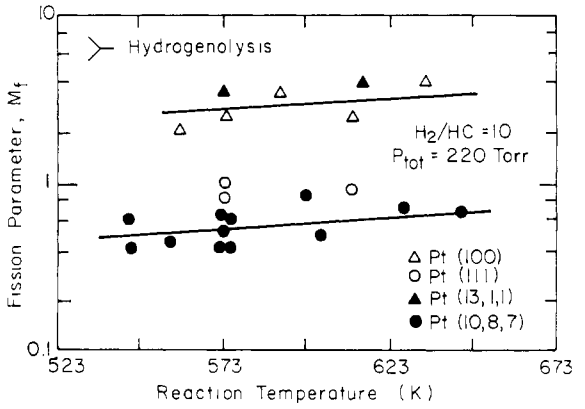

Figure 6. Fission parameters determined as a function of reaction temperatures for isobutane hydrogenolysis catalyzed over platinum single-crystal surfaces.

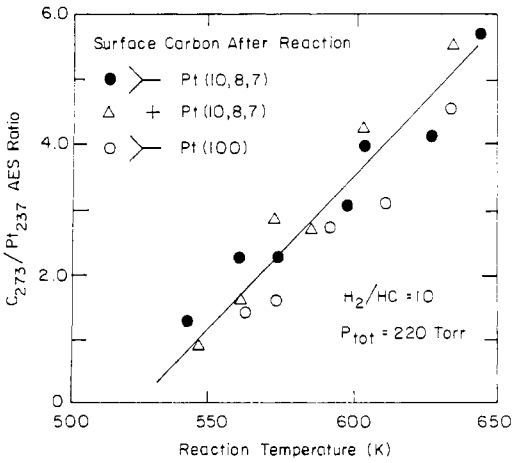

Figure 7. Temperature dependence of the C_{273}/Pt_{237} AES peak-to-peak height ratio measured following isobutane and neopentane reaction studies over Pt(100) and Pt(10,8,7).

using $M_f = (2[C_2] + [C_3])/[C_1]$ are shown in Figure 6. The concentrations of hydrogenolysis products with i carbon atoms are represented by $[C_i]$. The (111), (332), (557), and (10,8,7) surfaces, that are mostly composed of hexagonal (111) microfacets, displayed fission parameters smaller than 1 under all reaction conditions. The (100) and (13,1,1) platinum surfaces, that are mostly composed of square (100) microfacets, always displayed fission parameters that were in the range 2–6. The (100) and (13,1,1) surfaces produced more *ethane* and less methane and propane as compared to the other platinum crystal faces. On the basis of the low conversions of these experiments (≤0.2% total), the relative rates of iso- and *n*-butane hydrogenolysis, and adsorption equilibrium constants reported by Maurel et al.,[15] the possibility that secondary reactions of *n*-butane produced in isomerization contribute to these distributions can be ruled out.

Auger analysis of the surface composition following the isobutane reaction studies always revealed the buildup of about one monolayer of strongly bound carbonaceous species. No ordering in this layer could be detected by LEED. The continuous deactivation that was observed for hydrogenolysis and isomerization catalyzed over all six surfaces indicates that at least a part of the carbonaceous deposit was bound irreversibly as a deacti-

(14) Fission parameters for hydrogenolysis reactions of hydrocarbons containing n carbon atoms are more generally expressed by

$$M_f = [C_1]^{-1}\sum_{i=2}^{n}\sum_{j}(n-i)[C_i]_j$$

where the sum over j includes all products with i carbon atoms. For further explanation, see V. Ponec and W. M. H. Sachtler, *Catal., Proc. Int. Congr., 5th*, 645 (1972).

(15) G. Leclercq, L. Leclercq, and R. Maurel, *J. Catal.*, **50**, 87 (1977).

Table IV. Initial Reaction Rates, Selectivities, and Carbon Coverages Measured for *n*-Butane Reactions Catalyzed over Pt(100), Pt(111), and Pt(13,1,1)[a]

catalyst	initial rates at 573 K, molec/Pt·atom·s (±20%) hydrog	isom	dehydrog	selectivity of isom, mol % 573 K	615 K	C/Pt[b] at 615 K
Pt(100)	0.0087	0.037	≳0.48	79	52	1.7
Pt(111)	0.0071	0.013	≳0.45	65	27	2.0
Pt(13,1,1)	0.0098	0.046	≳0.48	82	56	2.7

[a] $H_2/HC = 10$, $P_{tot} = 220$ torr. [b] Carbon atoms per surface platinum atom (±25%).[8,13]

vating residue. The rate of deactivation was similar for both reactions and appeared to be independent of surface structure (Figure 3). The rate of deactivation increased markedly with increasing temperature, and this was accompanied by an increased surface coverage by carbonaceous species. Figure 7 summarized C_{273}/Pt_{237} AES peak-to-peak height ratios measured following isobutane and neopentane reaction studies on the (100) and (10,8,7) platinum surfaces. These peak height ratios can be converted into approximate (±25%) atomic ratios expressed as carbon atom equivalents per surface platinum atom by multiplying by 0.74 for Pt(100)[8] and 0.62 for Pt(10,8,7),[13] respectively. With these conversions it follows that the surface coverage by carbonaceous species was equivalent to 1–4 carbon atoms per surface platinum atom.

Several different kinetic models were investigated to describe the deactivation kinetics. At the lowest temperatures studied (540–640 K), the deactivation was well described by a simple first-order model whereas at higher temperatures the deactivation displayed a fractional-order time dependence, i.e.; $R(t) = R(t = 0)\exp(-\alpha t^n)$, $n \leq 1$. Best-fit orders for the deactivation reaction were determined from order plots (not shown) of ln (ln $R(t)$ − ln $R(t = 0)$) vs. ln t. These values decreased from 0.8–1.0 at 540–560 K to 0.4–0.6 at 620–640 K. The apparent activation energy for deactivation was estimated from the initial slopes of deactivation plots testing first- and half-order deactivation models.[8] Arrhenius plots for the deactivation rate constant (α) yielded apparent activation energies that were in the range 12–19 kcal/mol independent of the deactivation model.[8]

***n*-Butane Reactions.** The isomerization, dehydrogenation, and hydrogenolysis of *n*-butane were investigated on the (100), (111), and (13,1,1) platinum surfaces at 573 K with $H_2/HC = 10$ and $P_{tot} = 220$ torr. Following a 70–90-min reaction time, the samples were heated to 615 K for an additional 40–60 min so that selectivities could be determined at a higher temperature. Initial turnover frequencies at 573 K, fractional isomerization selectivities at 573 and 615 K, and surface carbon coverages determined following the reactions at 615 K are summarized in Table IV. Isomerization of *n*-butane at 573 K displayed substantial structure sensitivity that was similar to that observed for isobutane isomerization. The (100) and (13,1,1) platinum surfaces exhibited isomerization activities that were at least three times higher than that for Pt(111); [Pt(13,1,1) ≈ Pt(100) > Pt(111)]. The hydrogenolysis reaction displayed little structure sensitivity [Pt(13,1,1) ≈ Pt(100) > Pt(111)] for the three surfaces investigated. The initial dehydrogenation rates reported in Table IV represent lower limits to the absolute dehydrogenation rates that could not be measured directly because of thermodynamic constraints. The dehydrogenation reactions produced equilibrium concentrations of 1-, *cis*-2-, and *trans*-2-butenes within about 20 min over all three surfaces.

Product distributions and fission parameters for *n*-butane hydrogenolysis are summarized in Table V. At 573 K, the (111) surface produced a statistical hydrogenolysis distribution whereas the (100) and (13,1,1) platinum surfaces displayed much higher selectivities for scission of the internal C–C bond.

Neopentane Reactions. The isomerization and hydrogenolysis of neopentane were investigated over the same platinum crystal surfaces under identical reaction conditions. Product accumulation

Table V. Product Distributions and Fission Parameters for *n*-Butane Hydrogenolysis Catalyzed over Platinum Single-Crystal Surfaces[a]

catalyst	*T*, K	hydrog dist, mol C_1	C_2	C_3	M_f
Pt(100)	573	23	58	19	5.9
	615	25	50	25	5.0
Pt(111)	573	40	30	30	2.2
	615	38	30	32	2.4
Pt(13,1,1)	573	33	49	28	3.5
	615	36	45	29	3.3

[a] $H_2/HC = 10$, $P_{tot} = 220$ torr.

Table VI. Initial Reaction Rates, Fractional Isomerization Selectivities, *n*-Pentane to Isopentane Ratios, and Surface Carbon and Sulfur Coverages Determined at 573 K for Neopentane Reactions Catalyzed over Platinum Single-Crystal Surfaces[a]

catalyst	initial rates, molec/Pt·atom·s isom	hydrog	selectivity of isom, mol %	*n*-C_5/*i*-C_5	C/Pt[b]	S/Pt[c]
Pt(100)	0.18	0.024	88	0.16	1.0	0.06
Pt(111)	0.11	0.015	87	0.03	1.9[d]	0.04[d]
Pt(13,1,1)	0.20	0.024	89	0.14	1.9[d]	0.05[d]
Pt(10,8,7)	0.20	0.026	88	0.02	1.0	0.06
Pt(332)	0.35	0.067	84	0.03	0.8	~0

[a] $H_2/HC = 10$, $P_{tot} = 220$ torr. [b] Carbon atoms per surface Pt atom (±25%).[8,13] [c] Sulfur atoms per surface Pt atom (±40%).[8] [d] At 615 K.

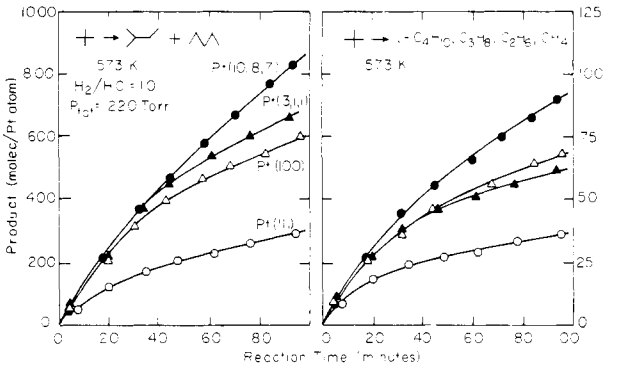

Figure 8. Product accumulation curves measured as a function of reaction time for neopentane isomerization (left) and hydrogenolysis (right) catalyzed at 573 K over platinum single-crystal surfaces.

curves determined as a function of reaction time at 573 K are compared for isomerization and hydrogenolysis in Figure 8. Initial reaction rates, selectivities, and surface carbon and sulfur coverages measured after the reactions are tabulated in Table VI. In contrast to the C_4 alkane reactions, surface structure had only a small influence on the initial rates and selectivities of neopentane isomerization. The fractional selectivity for isomerization was always in the range 84–89%, and the difference in initial rates between the least-active (111) and most-active (332) platinum surfaces was only about a factor of 2–3 for both isomerization and hydrogenolysis. The selectivity in isomerization for *n*-pentane production was the only feature of the neopentane reaction chemistry that displayed notable structure sensitivity. While the (111), (332), and (10,8,7) platinum surfaces yielded only 2–3% *n*-pentane in isomerization, the (100) and (13,1,1) surfaces produced 12–14% *n*-pentane. Thus, since again the probability for a secondary reaction is very low, *the (100) and (13,1,1) surfaces displayed a marked preference for two consecutive rearrangements during a single residence on the surface.*

Arrhenius plots for neopentane hydrogenolysis and isomerization catalyzed on the (10,8,7) platinum surface are compared in Figure 9. For temperatures below about 600 K, both reaction pathways

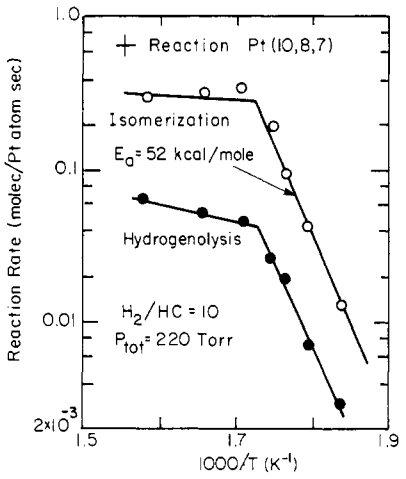

Figure 9. Arrhenius plots for neopentane isomerization and hydrogenolysis catalyzed over Pt(10,8,7).

Table VII. Initial Product Distributions and Fission Parameters for Neopentane Hydrogenolysis Catalyzed on Platinum Single-Crystal Surfaces[a]

		hydrog dist, mol				
catalyst	T, K	C_1	C_2	C_3	i-C_4	M_f
Pt(100)	573	39	13	15	33	2.7
Pt(111)	573	49	5	4	42	1.3
	615	45	12	15	28	2.2
Pt(13,1,1)	573	40	11	13	36	2.5
	615	31	24	23	22	4.5
Pt(10,8,7)	543	58	4	11	27	1.0
	573	58	4	6	32	1.0
	604	51	7	16	26	1.6
Pt(332)	573	58	6	6	30	1.0

[a] H_2/HC = 10, P_{tot} = 220 torr; n-butane production could not be accurately measured.

displayed normal Arrhenius behavior with high activation energies in the range 50–55 kcal/mol. At higher temperatures, no further increase in initial rates was detected. As for the isobutane reactions, the rate of deactivation increased with increasing reaction temperature. Deactivation was accompanied by the deposition of about one monolayer of strongly chemisorbed carbonaceous species (Table VI, Figure 7).

Fission parameters and initial product distributions for neopentane hydrogenolysis are compared at several temperatures in Table VII. The (100) and (13,1,1) crystal faces produced much more ethane and propane and less methane as compared to the other platinum surfaces. Consequently, the fission parameters were largest for the (100) and (13,1,1) platinum surfaces.

Discussion

Structure Sensitivities of Alkane Skeletal Rearrangement. A. Isomerization. Significant differences in isomerization activity were detected for platinum single-crystal surfaces with different atomic structures. Figure 10 summarizes initial rates as a function of crystallographic orientation for n-butane, isobutane, and neopentane isomerization catalyzed at 573 K. Isobutane and n-butane isomerization displayed maximum rates on the (100) and (13,1,1) platinum surfaces that were at least three–five times higher than the rates of the same reactions catalyzed over Pt(111), Pt(332), Pt(557), and Pt(10,8,7). High concentrations of (100) microfacets were required for high catalytic activity in butane isomerization. By contrast, neopentane isomerization activity displayed little dependence on platinum surface structure. This difference may be related to the fact that sulfur contamination was detected by AES *only* after the neopentane reaction studies. While the sulfur contamination was always small (3–6% of a monolayer),[8] it could likely alter the structure sensitivity of this reaction pathway. Since olefin intermediates could not form during neopentane reactions prior to skeletal rearrangement, different degrees of substitution

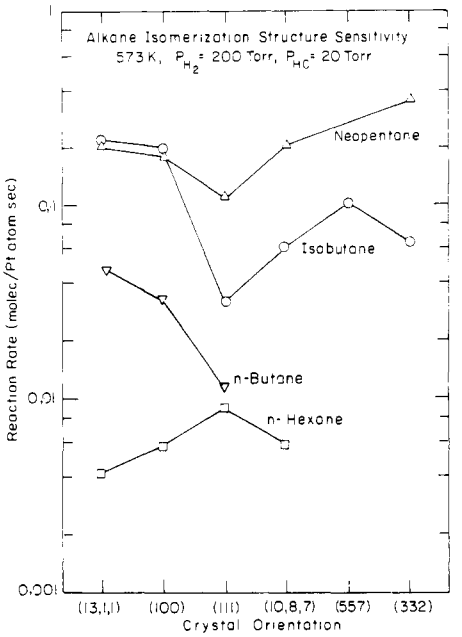

Figure 10. Structure sensitivities of alkane isomerization reactions catalyzed over platinum single-crystal surfaces.

for the reacting hydrocarbons could also contribute to the different structure sensitivites for neopentane and butane isomerization. Olefin formation occurred readily during isobutane and n-butane reaction studies.

Results for n-hexane isomerization catalyzed over the same platinum surfaces are also included in Figure 10. The absence of structure sensitivity for this reaction has been discussed[16] in terms of an isomerization mechanism that was dominated by C_5 cyclic intermediates. These intermediates were not possible during light-alkane skeletal rearrangement.

The order of isomerization activities at 573 K for the different hydrocarbons followed the sequence neopentane ≥ isobutane > n-butane > n-hexane. While this order varied slightly with surface structure, it tends to indicate that isomerization rates increase with increasing degree of substitution and decreasing molecular weight. Further studies using additional hydrocarbons would be worthwhile to confirm this correlation.

The structure sensitivities reported here for butane isomerization compare favorably with results reported by Anderson and Avery[1] for the same reactions catalyzed under similar conditions over oriented platinum films with (100) and (111) surface structure (T = 540–580 K, H_2/HC = 12, P_{tot} = 48 torr). These workers observed higher isomerization activities on the oriented (100) films, and the differences in rates between (111) and (100) films were comparable to those described here for single-crystal surfaces. Table VIII compares catalytic activities and selectivities determined in this research at 573 K with those reported for oriented films and other types of platinum catalysts, e.g., unoriented films, powders, and Pt/SiO_2. The initially clean single-crystal surfaces consistently displayed much higher catalytic activities than those reported for other types of platinum catalysts.

The absence of significant structure sensitivity for neopentane isomerization appears to be in good agreement with results reported by Foger and Anderson[19] for neopentane reactions catalyzed at 530–600 K over Pt/SiO_2 catalysts. While isomerization selectivity increased significantly in their studies when the average metal particle size was varied between 10 and 70 Å, the isom-

(16) S. M. Davis, F. Zaera, and G. A. Somorjai, *J. Catal.*, in press.
(17) R. S. Dowie, D. A. Whan, and C. Kemball, *J. Chem. Soc., Faraday Trans. 1*, **68**, 2150 (1973).
(18) L. Guczi, A. Sarkany, and P. Tetenyi, *J. Chem. Soc., Faraday Trans. 1*, **70**, 1971 (1974).
(19) K. Foger and J. R. Anderson, *J. Catal.*, **54**, 318 (1978).
(20) M. Boudart, A. W. Aldag, L. D. Ptak, and J. E. Benson, *J. Catal.* **11**, 35 (1968).

Table VIII. Comparison between Model and Practical Catalysts for Light-Alkane Skeletal Rearrangement Reactions

catalyst	H_2/HC	P_{tot}, torr	T, K	total rate,[a] molec/Pt·atom·s	selectivity of isom,[b] mol %	ref
			Isobutane Reaction			
Pt(100)	10	220	573	0.23	98	
Pt(111)	10	220	573	0.036	90	
Pt film (100)	12	48	573	0.011	59	1
Pt film (111)	12	48	573	1.3×10^{-3}	83	1
Pt film	11.5	38	633	~0.03	73	17
Pt powder	20	210	650	$\sim 4 \times 10^{-4}$	73	18
			n-Butane Reaction			
Pt(100)	10	220	573	0.047	79	
Pt(111)	10	220	573	0.020	65	
Pt film (100)	12	48	573	0.020	16	1
Pt film (111)	12	48	593	9×10^{-3}	40	17
Pt film	11.5	38	573	7×10^{-4}	22	18
			Neopentane Reaction			
Pt(100)	10	220	573	0.20	88	
Pt(111)	10	220	573	0.13	87	
Pt/SiO_2	20	760	573	~0.014	36	19
(d = 10 Å)	20	760	573	~0.014	36	19
(d = 40 Å)	20	760	573	~0.023	47	19
(d = 70 Å)	20	760	573	~0.013	60	19
Pt/Al_2O_3 (D = 0.73)	10	760	580	5×10^{-3}	60	20
Pt/SiO_2 (D = 0.17)	10	760	580	0.017	23	20
Pt powder ($D \sim 10^{-2}$)	10	760	580	8×10^{-4}	90	20

[a] Isomerization plus hydrogenolysis. [b] $S_{isom} = R_{isom}/(R_{isom} + R_{hydrog})$.

erization rates changed by only a factor of 2 with no clear correlation with average metal particle size.

Our results indicate that the structure sensitivity of alkane isomerization depends markedly upon the structure of the reacting hydrocarbon. When structure sensitivity was detected, it originated primarily from the atomic structure of the (100) or (111) terraces. The effect of steps and kinks, that were present in high concentrations on the (13,1,1), (332), (557), and (10,8,7) platinum surfaces, was to increase the isomerization rates, although this effect was small as compared to the changes introduced by terrace structure. The structure sensitivity of isobutane isomerization diminished rapidly with increasing reaction temperature.

B. Hydrogenolysis. Hydrogenolysis activities determined as a function of crystallographic orientation at 573 K are compared for isobutane, *n*-butane, neopentane, and *n*-hexane in Figure 11. Hydrogenolysis rates for *n*-butane and *n*-hexane displayed little dependence on platinum surface structure for the flat crystal faces investigated. However, at 573 K, the stepped and kinked platinum surfaces with (111) terraces were several times more active than the flat low-index crystal faces for isobutane and neopentane hydrogenolysis. At lower reaction temperatures, step and kink sites were uniquely effective for these C–C bond-breaking reactions. However, these differences in hydrogenolysis rates appeared to decrease sharply with increasing reaction temperature (Figure 4). Differences in hydrogenolysis activities for hydrocarbons with different structure were substantially smaller than those for the competing isomerization reactions.

C. Selectivity. The light-alkane reaction studies have confirmed that platinum is an excellent dehydrogenation catalyst.[9] Whenever dehydrogenation was possible (isobutane, *n*-butane, *n*-hexane), this reaction pathway was at least 3–50 times faster than the sum rate of all skeletal rearrangement reactions. Under our conditions (H_2/HC = 10, T = 540–640 K), hydrogenation–dehydrogenation equilibrium was established within minutes over all platinum surfaces.

At lower reaction temperatures (≤570 K), the initially clean platinum single-crystal surfaces displayed very high selectivities for isomerization vs. hydrogenolysis. These selectivities are compared in Table VIII with those reported previously for other types of platinum catalysts. The single-crystal surfaces consistently displayed higher isomerization selectivities than practical catalysts. A maximum isomerization selectivity of about 98% was observed for isobutane isomerization catalyzed over Pt(100) at 560 K. At

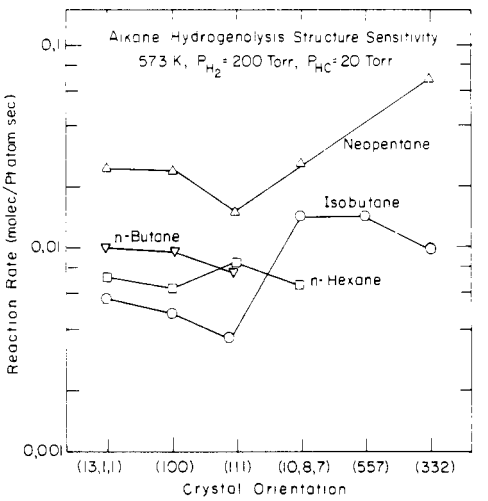

Figure 11. Structure sensitivities of alkane hydrogenolysis reactions catalyzed over platinum single-crystal surfaces.

573 K, the isomerization selectivities decreased in the order isobutane ≥ neopentane > *n*-butane. Selectivities for *n*-butane and isobutane isomerization decreased markedly with increasing temperature, although with neopentane, the selectivity displayed little temperature dependence.

The drastic changes in butane isomerization selectivity with increasing temperature can best be explained if (1) a common surface intermediate exists for both reaction pathways but the activation energy for hydrogenolysis is higher than that required for isomerization (as observed) or (2) hydrogenolysis and isomerization result from surface intermediates with different hydrogen content (composition); hydrogenolysis intermediates have lower hydrogen content and are favored at high temperatures. Both effects probably operate simultaneously. The fact that isobutane isomerization catalyzed on the (100) platinum surface displayed a maximum rate at about 590 K suggests strongly that explanation (2) is appropriate in this case.[8,16]

The fractional selectivity for neopentane isomerization was always in the range 78–90%, independent of platinum surface structure and the reaction temperature. These selectivities are compared in Table VIII with those reported by Foger and An-

derson,[19] who noted that isomerization selectivity for Pt/SiO_2 catalysts increases with increasing average metal particle size. A limiting selectivity of about 90% was proposed for platinum surfaces that consist entirely of (111) microfacets. Significantly, our results clearly show that *high isomerization selectivity is not restricted to (111) surfaces. All initially clean platinum surfaces that contain high concentrations of contiguous (111) or (100) microfacets display very high isomerization selectivity.*

The selectivity for *n*-pentane production during neopentane reaction studies displayed a marked dependence on platinum surface structure. This unique reaction required two consecutive rearrangements during a single residence on the platinum surface. It occurred readily only on the (100) and (13,1,1) platinum surfaces that contained high concentrations of square (100) microfacets. In this case consecutive rearrangement accounted for about 15% of the total isomerization activity. Since the structure sensitivity of this reaction closely paralleled that for isobutane isomerization, it appears likely that isopentane intermediates are important in the reaction pathway leading to multiple rearrangement. Muller and Gault[21] have previously reported that consecutive rearrangements take place readily during isomerization reactions of dimethylbutanes catalyzed at 540–570 K over platinum films.

D. Hydrogenolysis Product Distributions. Large differences in hydrogenolysis selectivity were detected for platinum single-crystal surfaces with different atomic structure. Hydrogenolysis of *n*-butane at 573 K was mainly characterized by single C–C bond-breaking events that were accompanied by 2–5% hydrocracking ($n\text{-}C_4 \rightarrow 4C_1$). Approximate C–C bond-rupture probabilities were

	Pt(100)	Pt(111)	Pt(13,1,1)
C_1-C_2	0.20	0.34	0.26
C_2-C_3	0.60	0.33	0.48
C_3-C_4	0.20	0.33	0.26

The (111) platinum surface lead to statistical C–C bond breaking whereas the (100) surface displayed a clear preference for scission of the internal C–C bond. The (13,1,1) surface with (111) steps and (100) terraces displayed intermediate behavior. Possible explanations for the different selectivities were proposed,[16] in connection with studies of *n*-hexane hydrogenolysis catalyzed over the same platinum surfaces, where a similar pattern of hydrogenolysis selectivity was detected.

A more complicated series of reaction steps involving multiple C–C bond-breaking events and skeletal rearrangement prior to hydrogenolysis was apparent during isobutane hydrogenolysis. The product distributions for Pt(111) and Pt(10,8,7) could be described by a series of successive demethylation processes where single C–C bond scission ($i\text{-}C_4 \rightarrow C_3 + C_1$) represented 65–80% of the total hydrogenolysis reaction. Similar product distributions were reported previously by Dowie,[17] Guczi,[18] Anderson[1] and co-workers for isobutane reactions catalyzed over platinum films. However, demethylation could only account for 45–55% of the hydrogenolysis products produced on the (100) and (13,1,1) platinum surfaces. In this case, ethane yields were always much too high to be represented by consecutive demethylation. Since conversions were always too low to allow for secondary reactions, a reasonable explanation for this unique hydrogenolysis selectivity appears to involve rearrangement to a surface intermediate with a linear structure like *n*-butane prior to hydrogenolysis; i.e.:

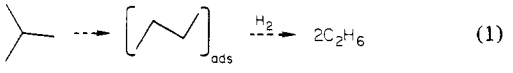

(1)

This process appears to be responsible for the unusually high fission parameters that were determined for isobutane hydrogenolysis catalyzed or the (100) and (13,1,1) platinum surfaces (Figure 5).

A similar analysis is applicable to neopentane hydrogenolysis, as in this case demethylation represented 75–90% of the reaction over Pt(111) and Pt(10,8,7) but only 65–75% of the reaction over Pt(100) and Pt(13,1,1). Over the (100) and (13,1,1) platinum surfaces, ethane and propane were produced in yields that were again too high to be accounted for by consecutive demethylation. The formation of these hydrogenolysis products is expected if skeletal isomerization precedes hydrogenolysis; i.e.:

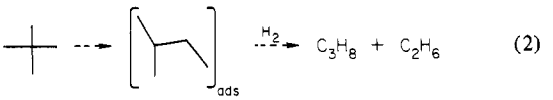

(2)

While the product distributions determined for neopentane hydrogenolysis on Pt(111) and Pt(10,8,7) compare closely with those reported previously for Pt films and Pt/SiO_2,[1,19] the product distributions for Pt(100) and Pt(13,1,1) appear to be unique to single-crystal surfaces with high concentrations of (100) microfacets.

E. Nature of the Bond-Shift Mechanism. A variety of one- and two-atom-site mechanisms have been postulated[1,20,22-27] for bond-shift rearrangement of small alkanes on platinum (or palladium). With one notable exception,[24] all the proposed single-atom-site mechanisms involved α,γ-adsorbed species that are heterogeneous analogues of platinocyclobutanes.[28,32] The latter compounds have attracted much interest because of their ability to undergo a facile skeletal rearrangement (reaction 3) that ap-

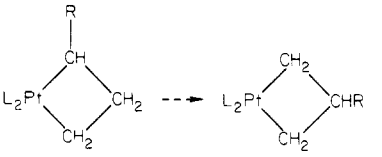

(3)

pears to be closely related to bond-shift isomerization[28,31,32] (L = pyridine, R = methyl,[31] phenyl[32]). Reaction pathways that were proposed for heterogeneous isomerization are summarized in Scheme I with isobutane taken as an example. Each pathway has been reviewed critically elsewhere.[25,33-35] The essential requirements of reactions 4, 6, and 7 are the transient existence of hydrocarbon intermediates with bridging methylene or methyl groups. Nonrigorous calculations[25,36] suggest that these species are stabilized by multicenter bonds as in (I) and partial charge

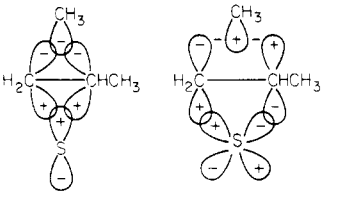

I

transfer from the adsorbed species to the metal. Photoemission studies of energy level shifts[37] and work function changes[38,39] that

(21) J. M. Muller and F. G. Gault, *Catal., Proc. Int. Congr. 5th*, 743 (1972).

(22) J. C. Prudhomme and F. G. Gault, *Bull. Soc. Chim.* Fr., 827 (1966).
(23) F. Garin and F. G. Gault, *J. Am. Chem. Soc.*, **97**, 4466 (1975).
(24) M. A. McKervey, J. J. Rooney, and N. G. Samman, *J. Catal.*, **30**, 330 (1973).
(25) J. K. A. Clarke and J. J. Rooney, *Adv. Catal.*, **25**, 125 (1976).
(26) J. M. Muller and F. G. Gault, *J. Catal.*, **24**, 361 (1972).
(27) F. G. Gault, V. Amir-Ebrahami, F. Garin, F. Parayre, and F. Weisang, *Bull. Soc. Chim. Belg.*, **88**, 475 (1979).
(28) P. Foley, R. DiCosimo, and G. M. Whitesides, *J. Am. Chem. Soc.*, **102**, 6713 (1980).
(29) C. P. Casey, D. M. Scheck, and A. J. Shusterman, *J. Am. Chem. Soc.*, **101**, 4233 (1979).
(30) T. H. Johnson and S. S. Cheng, *J. Am. Chem. Soc.*, **101**, 5277 (1979).
(31) R. J. Al-Essa, R. J. Puddephatt, P. J. Thompson, and C. F. H. Tipper, *J. Am. Chem. Soc.*, **102**, 7546 (1980).
(32) R. J. Al-Essa, R. J. Puddephatt, M. A. Quayser, and C. F. H. Tipper, *J. Am. Chem. Soc.*, **101**, 364 (1979).
(33) J. M. Dartigues, A. Chambellan, S. Corolleur, F. G. Gault, A. Renouprez, B. Moraweck, P. Bosch Giral, and G. Dolmai-Imelik, *Nouv. J. Chim.*, **3**, 591 (1979).
(34) J. R. Anderson, *Adv. Catal.*, **23**, 1 (1973).
(35) V. Ponec, in "The Chemical Physics of Solid Surfaces and Heterogeneous Catalysis", Elsevier, Amsterdam, 1981, Vol. 4.
(36) J. R. Anderson and N. R. Avery, *J. Catal.*, **7**, 315 (1967).
(37) See for example, J. E. Demuth and D. E. Eastman, *Phys. Rev. Lett.*, **32**, 1123 (1974).

Scheme I

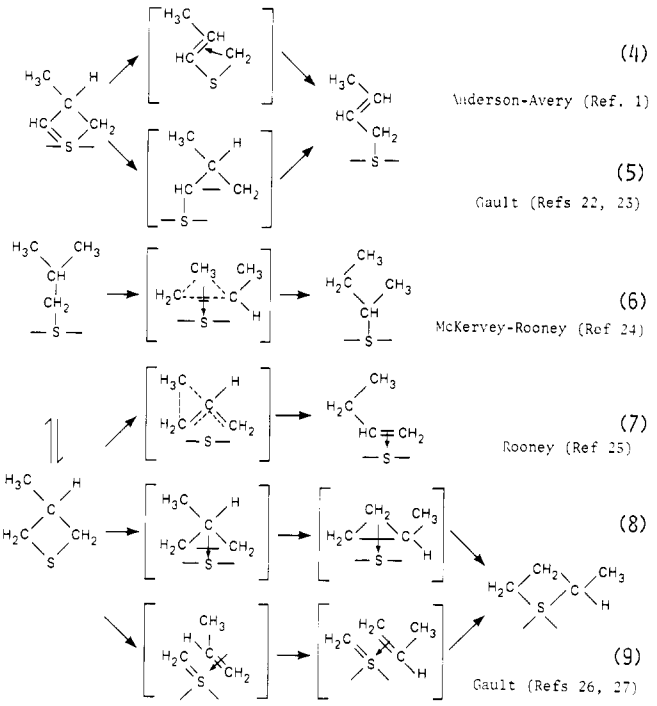

accompany hydrocarbon chemisorption have shown that charge transfer does take place, that it is particularly marked in the case of platinum, and that it is reasonable in this case to think of surface intermediates with partial carbonium ion character.[8]

The question naturally arises whether the structure sensitivities reported here for iso- and *n*-butane isomerization can be related to any of the previously proposed reaction mechanisms. The answer appears to be yes. The (100) and (13,1,1) platinum surfaces have accessible d (and p) orbitals that emerge from the surfaces with appropriate angles and symmetries to form half-reaction states like that depicted in (I). However, in the absence of extensive sp–d hybridization, the (111) surface, and the terraces of the (332), (557), and (10,8,7) platinum surfaces do not possess such easily accessible orbitals. This is shown in Figure 12, which compares the directions of emergence of the t_{2g} and e_g orbitals from the (100) and (111) surfaces of an fcc metal.[40] Only those orbitals that project out of the surface planes are indicated. The widths, positions, and occupancies of the d bands that correspond to these orbitals have been considered explicitly elsewhere.[5] The important points are that (1) the indicated d-orbital symmetries are maintained at the surface, (2) the d orbitals can be accurately regarded as localized, quasi-atomic-like in character[41], and (3) neither d band is completely filled, i.e., both types of d orbitals are suitable for bonding with adsorbates. The (100) platinum surface has an e_g orbital projecting normal to the crystal face and t_{2g} orbitals that emerge at 45° that are most suitable for the formation of intermediates with structures like (I). By contrast, the (111) platinum surface has no d (or p) orbitals that project either normal to the surface or in the direction of nearest neighbors. In this case, strong metal–hydrocarbon interaction appears to require σ-bonded surface species where a carbon atom becomes "nested" in the threefold hollow sites as observed for the stable ethylidyne, propylidyne, and butylidyne surface species ($Pt_3 \equiv C\text{–}R$, R = CH_3, C_2H_5, C_3H_8) chemisorbed on Pt(111).[42,43] Stabilization of bridging species like (I) on Pt(111) requires a more

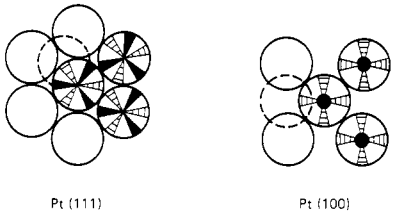

Figure 12. Representations of the d orbitals emerging from the (111) and (100) surfaces of an fcc metal (after bond[40]). Darkened regions represent e_g orbitals that emerge at 36° and 90° with respect to the surface plane for Pt(111) and Pt(100), respectively. Cross-hatched regions correspond to t_{2g} orbitals that emerge at 54° and 45° with respect to the surface for Pt(111) and Pt(100), respectively. Not shown are in plane t_{2g} orbitals that are directed toward nearest neighbors and in plane e_g orbitals that are directed toward next-nearest neighbors (Pt(100)).

complex bonding interaction involving linear combinations of t_{2g} orbitals centered on two or more metal atoms. Stepped and kinked platinum surfaces always have orbitals with appropriate symmetries for the formation of bridging intermediates. Thus, it is not surprising that stepped and kinked surfaces with (111) terraces are more active than Pt(111) but less active than Pt(100).

The actual situation for the surface electronic structure under reaction conditions is probably more complex than that suggested by this simplistic model which, nevertheless, can help to guide one's thinking. Local crystal-field effects at the surface determine the occupations of the individual d bands, which generally differ from those for the bulk.[44,45] Recent ab initio calculations for nickel surfaces, for example, revealed that the surface d bands are narrowed and more completely filled as compared to the corresponding bulk d bands.[45] Moreover, s–d hybridization appeared to become pronounced in the vicinity of the Fermi energy.[45] Such hybridization might result in the production of new surface orbitals that are uniquely suited for catalysis of bond-shift rearrangement.

F. Deactivation Kinetics and Formation of Surface Carbon. The light-alkane reaction-rate studies were always accompanied by continuous deactivation. Deactivation resulted from the formation of strongly bound surface-carbon deposits on the platinum surfaces.[46] Deactivation rates (carbon coverages) displayed little dependence on surface structure and increased with increasing temperature. The deactivation kinetics for isobutane and neopentane reactions catalyzed over Pt(100) and Pt(10,8,7) were correlated with the empirical rate expression $R_t = R_0 \exp(-\alpha t^n)$ where the order parameter n decreased from 1 at 550–570 K to about 0.5 at 610–640 K. A possible explanation for these deactivation kinetics was discussed in connection with *n*-hexane reaction studies on the same six platinum surfaces.[16] The change in apparent order for the deactivation reaction was related to a change in the morphology of the carbonaceous deposit from two dimensional at low temperatures to three dimensional at high temperatures. The same conclusion appears to be applicable to the light-alkane reaction studies. A significant difference in deactivation behavior between the light-alkane and *n*-hexane reaction studies was in the amount of carbon deposited. At any given temperature, less carbon was deposited during light-alkane reaction studies, although this difference became small at high temperatures. Also, during the *n*-hexane reaction, the carbonaceous deposit that forms covers the defects (steps and kinks) preferentially over terraces, while in the case of reactions with light alkanes, both the defect and the terrace sites are covered with roughly equal probability.

Acknowledgment. This work was supported by the Director, Office of Energy Research, Office of Basic Energy Sciences, Materials Sciences Division of the U.S. Department of Energy, under Contract DE-AC03-76SF00098.

Registry No. Isobutane, 75-28-5; *n*-butane, 106-97-8; neopentane, 463-82-1; platinum, 7440-06-4.

(38) J. L. Gland, Ph.D. Thesis, University of California, Berkeley, 1973.
(39) P. E. C. Franken and V. Ponec, *Surf. Sci.*, **53**, 341 (1975).
(40) G. C. Bond, *Discuss. Faraday Soc.*, **41**, 200 (1966).
(41) See for example, S. G. Louie, *Phys. Rev. Lett.*, **40**, 1525 (1978); **42**, 476 (1979).
(42) L. L. Kesmodel, L. H. Dubois, and G. A. Somorjai, *J. Chem. Phys.*, **70**, 2180 (1979).
(43) R. J. Koestner, J. C. Frost, P. C. Stair, M. A. Van Hove, and G. A. Somorjai, *Surf. Sci.*, in press.
(44) P. H. Citrin and G. K. Wertheim, *Phys. Rev. Lett.*, **41**, 1425 (1978).
(45) J. Tersoff and L. M. Falicov, *Phys. Rev. B: Condens. Matter*, in press.
(46) S. M. Davis, F. Zaera, and G. A. Somorjai, *J. Catal.*, in press.